Closure to “Effect of Seepage-Induced Nonhydrostatic Pressure Distribution on Bed-Load Transport and Bed Morphodynamics” by

Discussion of "Transition between Two Bed-Load Transport Regimes: Saltation and Sheet-Flow" by P. Gao

March 2008, Vol. 134, No. 3, pp. 340–349.
DOI: 10.1061/(ASCE)0733-9429(2008)134:3(340)

Benoît Camenen[1]
[1]Cemagref UR HHLY, 3 bis quai Chauveau, CP 220, 69336 LYON cedex 09, France. E-mail: benoit.camenen@cemagref.fr

The author presented an interesting theoretical model for predicting the onset of the sheet-flow regime. It introduces the parameter P_b, which characterizes the proportion of grains moved from the surface layer. The proposed relationship for P_b is however derived from the bed-load formula by Abrahams and Gao (2006), which yields a nearly constant Shields parameter $\theta_t \approx 0.5$, a curious result that merits discussion.

Model for Bed-Load Transport

From the hypothesis proposed by the author, P_b is directly related to the volumetric bed-load transport rate q_b and the mean grain velocity U_b [Eq. (3) in the paper]. As all further developments to estimate q_b and U_b are based on the work by Abrahams and Gao (2006), the proposed equation for P_b appears to be a different way to write the bed-load formula originally proposed by Abrahams and Gao. Using the dimensionless bed load transport Φ and the definition of the Shields parameter $\theta = R_h S/[(s-1)D] = u_*^2/[(s-1)gD]$ (see Gao's paper for the notations; S is introduced here for the energy slope, R_h is the hydraulic radius, u_* is the shear velocity, and $s = \rho_s/\rho$ is the relative density of the sediment), Eqs. (10) and (12) in the paper yield

$$\Phi_b = \frac{q_b}{\sqrt{(s-1)gD^3}} = \frac{C_0 P_b U_b}{\sqrt{(s-1)gD}} = \frac{\theta u}{\sqrt{(s-1)gD}}\left(1 - \frac{\theta_c}{\theta}\right)^{3.4}$$
$$= \theta^{3/2}\frac{u}{u_*}G^{3.4} \tag{1}$$

which is exactly the equation proposed by Abrahams and Gao [2006, Eq. (25)].

Abrahams and Gao (2006) argued that the excess bed shear stress is balanced by intergranular collisions force and fluid drag/lift force, which may be written in a dimensionless form: $\theta - \theta_c = \theta_{tg} + \theta_{tf}$. Bagnold (1966) introduced a bed-load transport model where most of the energy is used to support the intergranular collisions force (θ_c and θ_{tf} assumed to be negligible)

$$\Phi_b = \frac{e_b}{\tan\alpha}\theta^{3/2}\frac{u}{u_*} \tag{2}$$

where e_b=bed-load efficiency. The angle of repose $\tan\alpha$ comes from the relationship $\theta_{tg} = \tan\alpha W'/[(\rho_s - \rho)gD]$ where W' is the immersed weight of the load. It explains the coefficient 0.6 in Gao's paper (the angle of repose for sands is usually taken as $\alpha \approx 30°$). Thus, Gao's developments are summarized as

$$P_b = \frac{\theta_{tg}}{C_0 \tan\alpha} \quad \text{while} \quad U_b = \frac{q_b \tan\alpha}{\theta_{tg} D} \tag{3}$$

For very low rates, θ_c is not negligible and $\theta_{tf} \gg \theta_{tg}$ (Bridge and Bennett 1992). When θ is close to θ_c, $\theta_{tg} \ll \theta$ and $P_b \to 0$; when $\theta \gg \theta_c$, $\theta_{tg} \approx \theta$ and $P_b = 1$ (inception of the sheet flow layer) yields thus to $\theta_{tg} \approx C_0 \tan\alpha = 0.4$. A link with Gao's results may be obtained using the empirical relationships suggested by Abrahams and Gao (2006): $\theta_{tg}/(\theta - \theta_c) = G^2$ and Eq. (12) for U_b. In that sense, P_b mainly expresses the effects of the critical Shields parameter on bed-load transport but not the transition between saltation and sheet flow regimes.

Effect of the Critical Shields Parameter on Bed-Load Transport

Estimating bed-load transport is challenging when θ_c is not negligible and $\theta - \theta_c \approx \theta_{tf}$. Following Meyer-Peter and Müller (1948), most authors add a factor that varies with the ratio $r_t = \theta_{cr}/\theta$ and assume $q_s = 0$ when $\theta < \theta_{cr}$. Camenen and Larson (2005) argued that the estimation of θ_c itself is subject to uncertainties, and then suggested an exponential function of θ/θ_{cr} (see Table 1).

For the experimental study used by Gao, side wall effects should have a significant influence on the estimation of the total shear stress applied to the bed as the width of the channel is narrow ($b = 0.1$ m) and velocities are large ($0.8 < u < 2.4$ m/s). As Gao seems to have used $R_h = h$ for his computations, the same assumption has been used below, but these results may differ significantly if a side wall correction is taken into account (*cf.* method of Vanoni and Brooks 1957).

In Table 1, the studied bed-load formulas are tested against Gao's data, and for each of these formulas, the ratio $\Phi/\theta^{3/2}$ is plotted versus the ratio $\theta/\theta_{cr} = 1/r_t$ in Fig. 1. The performance of the Abrahams and Gao (2006) formula is weaker than those provided by the Meyer-Peter and Müller (1948) or Camenen and Larson (2005) formulas. The Abrahams and Gao formula tends to overestimate bed load rates for the data with $D = 1.16$ mm and underestimate bed load rates for the data with $D = 7$ mm. As the equation for P_b is closely related to the Abrahams and Gao formula, its prediction capability may also be uncertain. The effect of the critical Shields parameter is also sharper using the Abrahams and Gao formula. r_t varying from 3 to 1.5 yields a decrease of bed load transport by a factor 10.6. For the Meyer-Peter and Müller and Camenen and Larson formulas, it yield a decrease by a factor 2.8 and 4.5, respectively.

Onset of the Sheet Flow Regime

For a fixed bed or very low bed-load rates, the flow resistance is generally related to the size of the bed material such as the roughness height $k_s \approx 2D$ (see Camenen et al. 2006). For the sheet flow regime, Wilson (1966) observed a linear relationship between k_s and θ. Sumer et al. (1996) observed however a more complex relationship where k_s is function of both D and θ. Camenen et al.

Table 1. Relationships for the Effect of the Critical Shields Parameter on the Bed-load Transport Rate and Statistical Results Compared to the Experimental Data by Guo

Author(s)	Meyer-Peter & Müller	Abrahams & Gao	Camenen & Larson
$\Phi/\theta^{3/2}$	$8(1-r_t)^{3/2}$	$u/u_*(1-r_t)^{3.4}$	$12\exp(-4.5r_t)$
$p_{\pm 1.5}$ (%)	79	38	79
mean[$\log(\Phi_{\text{pred.}}/\Phi_{\text{meas.}})$]	−0.092	+0.100	+0.007
std[$\log(\Phi_{\text{pred.}}/\Phi_{\text{meas.}})$]	0.37	0.72	0.31

Note: $p_{\pm 1.5}$ corresponds to the percentage of data correctly predicted within a factor 1.5 allowed.

(2006) and Recking et al. (2008) showed that k_s may be a function of θ or of q_b not only in the sheet- flow regime but also for relatively intense bed load rates. Camenen et al. (2006) suggested a critical Shields parameter $\theta_{cr,ur}$, up to which the ratio k_s/D increases with θ (see Fig. 2). $\theta_{cr,ur}$ was found to be a function of the Froude number and a dimensionless settling velocity. In Fig. 2, k_s, calculated based on Nikuradse's resistance relationship (*cf.* Camenen et al. 2006), is plotted against θ using Gao's experiments. For $D=7$ mm, there is an increase of k_s/D with θ, which is roughly predicted by the Camenen et al. model. On the contrary, for $D=1.16$ mm, k_s/D is a decreasing function of θ. How could it be explained? For this material, Gao observed a value for $\theta_t \approx 0.5$. And for $\theta > \theta_t$, he observed an increasing thickness δ_s of the sheet flow layer with θ. As $k_s \approx \delta_s$ (Wilson 1966), these results seem surprising.

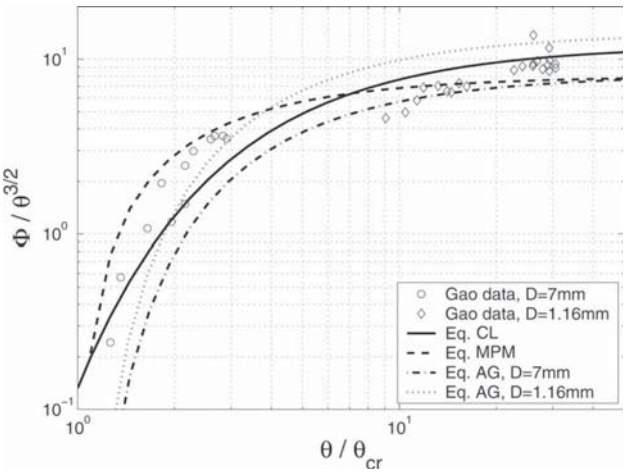

Fig. 1. Effect of the critical Shields parameter on the bed load transport rate using the Meyer-Peter and Müller, Abrahams and Gao, and Camenen and Larson formulas

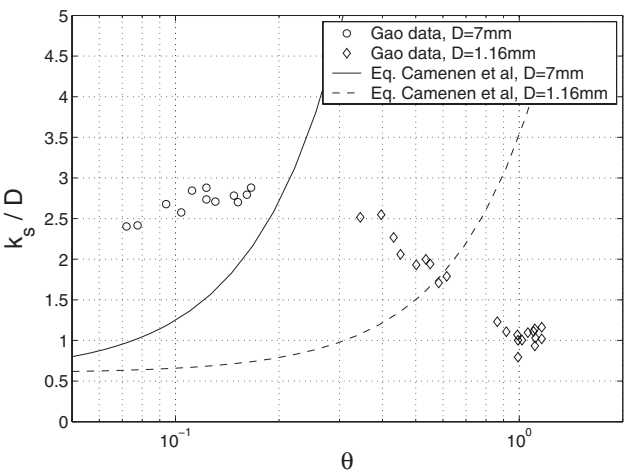

Fig. 2. Estimation of the roughness ratio k_s/D as a function of the Shields parameter

Although the theoretical aspects of the model suggested by Gao are of much interest, the final relationship presents some weaknesses. The model yields a nearly constant value for the onset of the sheet flow regime ($\theta_t \approx 0.5$), whereas values found in the literature are often larger ($0.8 < \theta_t < 1.0$ for sheet flow regime with fine sediments). It has not been validated with other data sets with different grain sizes, and looking at his own data with $D=7$ mm, one may wonder if the model is valid, even if no sheet flow was apparently observed. The suggested formula for P_b significantly depends on the bed load model by Abrahams and Gao, which yields relatively poor results for the prediction of the bed load rates. Lastly, this model hypothesizes a direct transition between saltation and sheet-flow regimes without bed forms occurring, which seems unrealistic (at least for fine sands). Thus, there are several reasons to believe this model may be of limited applicability.

References

Abrahams, A., and Gao, P. (2006). "A bed-load formula transport model for rough turbulent open-channel flows on plane beds." *Earth Surf. Processes Landforms*, 31(7), 910–928.

Bagnold, R. (1966). "An approach of sediment transport model from general physics." *Technical Report 422-1*, U.S. Geol. Survey Prof. Paper, Reston, Va.

Bridge, J., and Bennett, S. (1992). "A model for the entrainment and transport of sediment grains of mixed sizes, shapes, and densities." *Water Resour. Res.*, 28(2), 337–363.

Camenen, B., Bayram, A., and Larson, M. (2006). "Equivalent roughness height for plane bed under steady flow." *J. Hydraul. Eng.*, 132(11), 1146–1158.

Camenen, B., and Larson, M. (2005). "A bedload sediment transport formula for the nearshore." *Estuarine Coastal Shelf Sci.*, 63(1–2), 249–260.

Meyer-Peter, E., and Müller, R. (1948). "Formulas for bed-load transport." *Proc., 2nd Meeting of the International Association for Hydraulic Structures Research*, pp. 39–64, IAHR, Delft, The Netherlands.

Recking, A., Frey, P., Paquier, A., Belleudy, P., and Champagne, J. (2008). "Bed-load transport flume experiments on steep slopes." *J. Hydraul. Eng.*, 134(9), 1302–1310.

Sumer, B., Kozakievicz, A., Fredsœ, J., and Deigaard, R. (1996). "Velocity and concentration profiles in the sheet-flow layer of movable bed." *J. Hydraul. Eng.*, 122(10), 549–558.

Vanoni, V., and Brooks, N. (1957). "Laboratory studies of the roughness and suspended load of alluvial streams." *Technical Rep.*, Sedimentation Lab., California Institute of Technology, Pasadena, Calif.

Wilson, K. (1966). "Bed-load transport at high shear stress." *J. Hydr. Div.*, 92(11), 49–59.

Closure to "Transition between Two Bed-Load Transport Regimes: Saltation and Sheet Flow" by Peng Gao

March 2008, Vol. 134, No. 3, pp. 340–349.
DOI: 10.1061/(ASCE)0733-9429(2008)134:3(340)

Peng Gao[1]
[1]Dept. of Geography, Syracuse Univ., Syracuse, NY 13244.

The writer thanks the discusser for raising several issues regarding the proposed model describing the transition between two bed-load transport regimes. It appears that further clarification on the results of this model is needed.

It is agreed that the theoretical expression for P_b [i.e., Eq. (7) in the original paper] was partly derived from the bed-load transport equation developed by Abrahams and Gao (2006), hereafter referred to as the AG equation. However, the original Eq. (7) is far more than a different version of the AG equation. First, P_b has a clear sedimentological meaning. It represents the proportion of grains in the top layer of the original mobile bed that is transported as bed load. Second, the original Eq. (7) is only valid for a limited range of values of $\boldsymbol{\theta}$ because P_b by definition cannot be greater than 1. In contrast, the AG equation applies to flows with any possible value of $\boldsymbol{\theta}$. Once $P_b=1$, the corresponding $\boldsymbol{\theta}$ value marks the hydraulic transition from the saltation to sheet-flow regime. This is the key theoretical idea demonstrated in the original paper and cannot be derived from the AG equation.

The discusser's Eq. (3) may be alternately derived in two steps. Combining the original Eq. (7) with $e_b=U_b/u\mathrm{G}$ and $\mathrm{G}=1-\theta_c/\theta$ (Abrahams and Gao 2006), and replacing q_b by the submerged bed-load transport rate $i_b=q_b(\rho_s-\rho)g$ lead to

$$P_b=\frac{i_b\left(1-\dfrac{\theta_c}{\theta}\right)}{e_bC_0D(\rho_s-\rho)gu} \tag{4}$$

Further combination of Eq. (4) with both Bagnold's energy equation $i_b\tan\alpha=e_b\omega$ (Bagnold 1966; 1973) and the definition of stream power $\omega=\tau u$ gives rise to

$$P_b=\frac{\theta-\theta_c}{C_0\,tan\,\alpha} \tag{5}$$

Comparison of Eq. (5) with the discusser's Eq. (3) indicates that the latter is a simplified form with an implied assumption that $\theta_{tg}\gg\theta_{tf}$. However, this assumption is only valid for high flow rates (i.e., $\theta\gg\theta_c$) under which bed-load grains are primarily supported by grain-to-grain collisions rather than by turbulent lift. Therefore, the discusser's concern is not justified for low flow rates. Additionally, when $\theta\gg\theta_c$, the discusser's conclusions that $\theta_{tg}\approx\theta$ and $P_b=1$ are erroneous, because the condition $\theta_{tg}\approx\theta$ is only valid when flows have extremely high θ values, which are greater than the threshold value of θ for the transition from saltation to sheet-flow regimes, θ_t. Thus, neither Eq. (5) nor the discusser's Eq. (3) is valid for flows with high θ values.

Moreover, the discusser's conclusion $\theta_t=C_0\tan\alpha=0.4$ assumes $\tan\alpha=0.6$. Abrahams and Gao (2006) showed, however, that this assumption is only valid for $\theta\gg\theta_t$. Therefore, use of $\tan\alpha=0.6$ to calculate θ_t is inappropriate.

The discusser further questions P_b by stating that it only reflects the effect of θ_c on bed-load transport. The proposed model for the transitional condition [i.e., Eq. (11) in the original paper] should be correctly used by setting $P_b=1$ and then calculating θ.

Table 1. Values of θ_t for Different θ_c

θ_c	0.01	0.02	0.03	0.04	0.05	0.06
θ_t	0.42	0.45	0.48	0.5	0.53	0.55

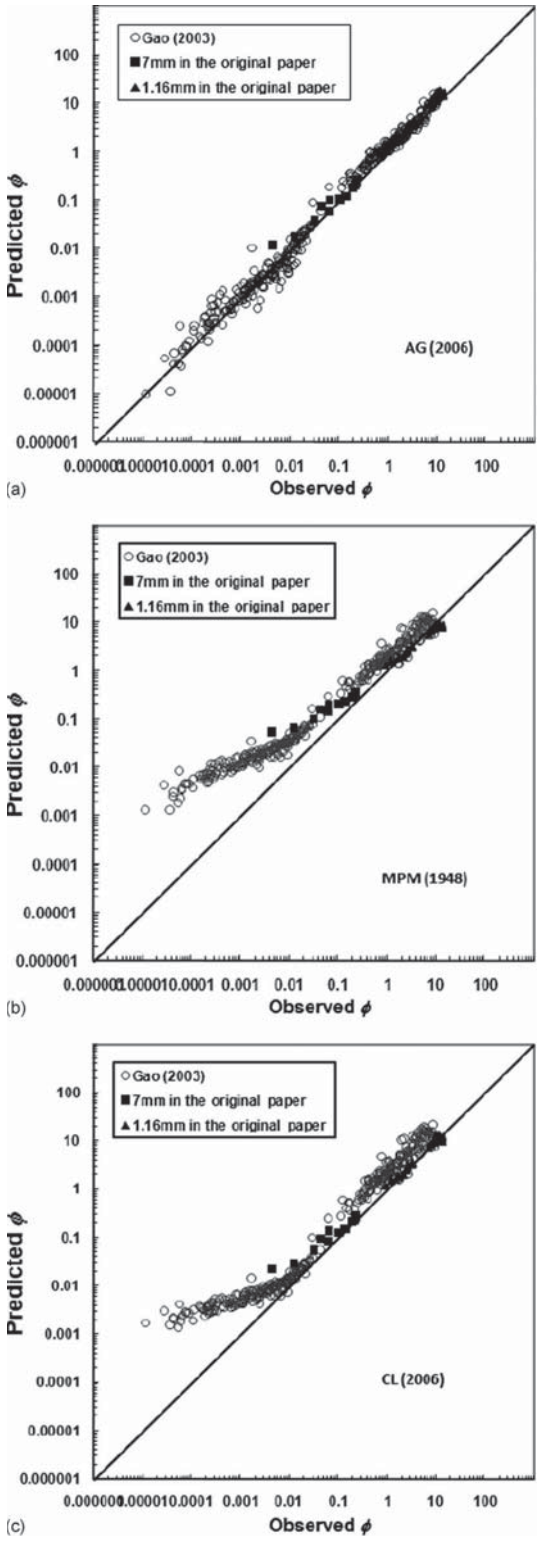

Fig. 1. Predicted ϕ against measured ϕ

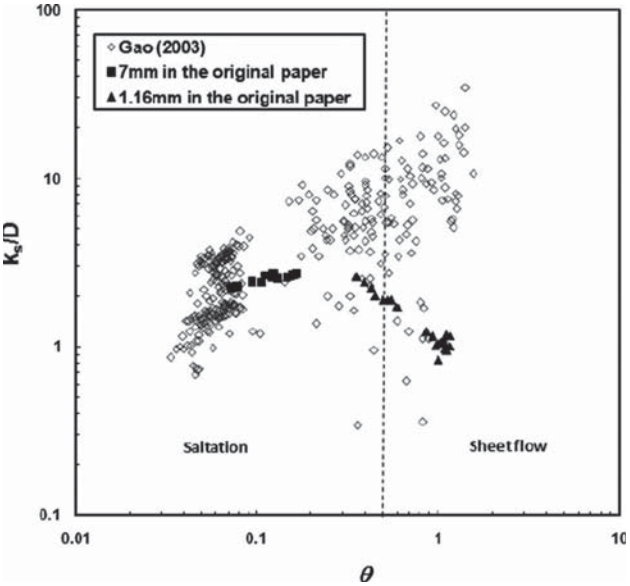

Fig. 2. Graph of k_s/D against θ

Because the original Eq. (11) contains θ_c, the calculated θ_t is affected by the value of θ_c, which is demonstrated in Table 1. When θ_c increases from 0.03 to 0.06 (i.e., 100%), θ_t merely changes from 0.48 to 0.55 (i.e., 17%). Therefore, any errors in determining θ_c (Buffington and Montgomery 1997) will have a limited effect on θ_t.

The discusser attributed the inaccuracy of the AG equation to the effect of θ_c on bed-load transport by suggesting in Fig. 1 in the discussion that this equation has the worst performance compared to the other two equations hereafter denoted as MPM (1948) and CL (2006). This comparison was based, however, on only a single data set, while the AG equation was developed using a group of data sets representing a wide range of hydraulic and sedimentological conditions [the original Eq. (11) was also developed from multiple data sets covering a broad range of hydraulic and sedimentological conditions]. A more broad-based comparison of predicted ϕ with the measured ϕ for the three equations selected by the discusser may be undertaken using the data sets complied in the original paper. Fig. 1 shows these results in which the data labeled Gao (2003) refer to those complied from published resources described in detail in Gao (2003). Although the CL equation predicts bed load transport rates better than the AG equation for data with grain size of 1.16 mm, the AG equation performs significantly better than either CL or MPM equations for the remainder of the large data set.

Finally, the discusser challenged the original Eq. (11) by arguing that the dimensionless roughness k_s/D should increase with θ, whereas for data with grain size of 1.16 mm, it decreases with θ (Fig. 2 in the discussion), which contradicts the empirical observation of bed-load layer thickness reported in the original paper. This conclusion is incorrect. First, the inverse relationship between k_s/D and θ exists in the sheet-flow regime (Fig. 2 in the discussion) wherein the discusser agrees that k_s is approximately equivalent to the bed-load layer thickness δ_s. However, several studies (Cheng 2003; Pugh and Wilson 1999; Sumer et al. 1996; Wilson 1989) have shown that δ_s/D is a linear function of θ, which means δ_s and hence k_s are independent of D in the sheet-flow regime. In contrast, k_s in Fig. 2 in the discussion was calculated using Nikuradse's resistance equation, which is affected by D. Therefore, this resistance equation is not valid in the sheet-flow regime for estimating k_s. Second, k_s as described in Camenen et al. (2006), is influenced by many factors such as grain size and density, setting velocity, and Froude number. Accordingly, it should be expected that for a given θ, k_s may have a wide range of numerical values. This is supported by the large scatter of the data in Fig. 2.

References

Bagnold, R. A., (1973). "The nature of saltation and of 'bed-load' transport in water." *Proc., R. Soc. Lond. A Math. Phys. Sci.*, 332, 473–504.

Buffington, J. M., and Montgomery, D. R., (1997). "A systematic analysis of eight decades of incipient motion studies, with spatial reference to gravel-bedded rivers." *Water Resour. Res.*, 33, 1993–2029.

Cheng, N.-S., (2003). "A diffusive model for evaluating thickness of bedload layer." *Adv. Water Resour.*, 26, 875–882.

Discussion of "Effect of Seepage-Induced Nonhydrostatic Pressure Distribution on Bed-Load Transport and Bed Morphodynamics" by Simona Francalanci, Gary Parker, and Luca Solari

April 2008, Vol. 134, No. 4, pp. 378–389.
DOI: 10.1061/(ASCE)0733-429(2008)134:4(378)

Tom E. Baldock[1] and Peter Nielsen[2]

[1]School of Civil Engineering, Univ. of Queensland, Brisbane, QLD 4072, Australia.

[2]School of Civil Engineering, Univ. of Queensland, Brisbane, QLD 4072, Australia.

The authors present a very interesting and useful paper on the effects of seepage on bed-load sediment transport and bed morphodynamics. Importantly, they consider the influence of the seepage on the free stream flow, which has been neglected in many previous studies. However, the discussers would like to note that the topic is not new and that substantial previous experimental work has been published in the fluvial and coastal sediment transport literature. The results presented by the authors are both consistent and inconsistent with this previous work. Furthermore, their modification to the Shields parameter [Eq. (39) in their paper] appears only partially complete, neglecting the influence of voids on the bulk seepage force that arises during seepage flow through a porous bed. In addition, a similar approach has previously been suggested by Nielsen (1998) and Baldock and Holmes (1999). More important perhaps, the pioneering steady flow work by Martin (1970), which was not considered by the authors, shows that the effects of seepage may have opposite effects depending on the character of the sediment. Nevertheless, the clear morphological differences observed by authors present clear evidence of a seepage effect, but we are not convinced that the full physics of the problem has yet been reconciled with all experimental observations. This paper is an attempt to broaden the discussion of seepage effects on sediment transport within the context of channel flows, uniform oscillatory flows, and nonuniform wave motion.

Since the work of Martin (1970), the other historical developments have been briefly as follows. In steady flows, Watters and Rao (1971) and Willets and Drossos (1975) found that seepage did not effect sediment motion, while Oldenziel and Brink (1974) did identify an influence. Löfquist (1975) investigated the possible importance of seepage flow in an oscillatory flow facility but the presence of ripples clouded the conclusions. However, during oscillatory water tunnel flow tests, Kruijt (1976) also found no significant seepage effects on sediment transport. Davis et al. (1993) performed field experiments into the stabilizing effect of lowering the watertable and enhancing downward seepage on beach morphodynamics. The effect was found to be too small to measure in the presence of other morphodynamic processes such as rip cell migration. Oh and Dean (1995) investigated the effects of an artificially elevated or lowered watertable behind the beach on beach erosion. The conclusions were unclear or contradictory. Field and laboratory investigations reported by Conley and Inman (1992, 1994) created renewed interest in seepage effects in coastal flows outside the swash zone. Nielsen (1998) suggested an adaptation of the Shields parameter along similar lines to those the authors proposed in their paper, which is discussed further below. Baldock and Holmes (1999) performed laboratory experiments under both steady flows and surface waves with both suction (seepage into the bed) and injection (seepage out of the bed), including fluidized bed conditions. No differences in threshold transport conditions were observed for steady currents, even over fluidized beds. Nielsen et al. (2001) performed sediment mobility experiments under waves using a horizontal sand bed, again with both injection and suction. The effects of even very strong seepage were found to be weak.

The authors note three effects of seepage on sediment transport: (1) the effect of seepage on bed shear stress; (2) the effect of seepage on immersed particle weight as used in the Shields parameter; and (3) the effect of seepage on the threshold of motion, as given by the critical Shields number. The effect of seepage on the shear stress can be further subdivided into two terms, one of which modifies the free stream flow through continuity and one which changes the boundary layer structure. The influence of suction or injection on boundary layer structure has long been known, and applied, in aeronautics (Turcotte 1960) and also identified for flows over sediment beds (Conley and Inman 1992; Chen and Chiew 2004). The authors ignore the possible influence of the seepage in directly modifying the bed shear stress in their model. However, very importantly, they include the continuity effect and demonstrate how this leads to strong secondary influences on the sediment transport, in their case through a backwater effect. To the discussers' knowledge, the continuity effect has not been considered in most of the experimental work cited above, and this neglect may explain some of the conflicting results.

In terms of the effect of seepage on immersed particle weight, this has been quantified by considering the additional nonhydrostatic pressure gradient acting within the pore water. However, both Nielsen (1998) and the authors neglected the porosity of the sediment within the bed material when determining the seepage force that modifies the effective bulk weight of the sediment. The correct critical hydraulic gradient, $i=i_c$, that induces piping, or fluidization, of a bed of sediment grains with density s and porosity n is

$$i_c = -(s-1)(1-n) \tag{1}$$

rather than simply $i_c=-(s-1)$, as is well known in soil mechanics (Smith 1968). The authors use the correct relationship for the critical hydraulic gradient, from Cheng and Chiew (1999), in their expression for the critical Shields number [their Eqs. (30) and (32)]. This is inconsistent with their Eqs. (16) and (39), which do not account for porosity.

Nielsen (1998) proposed that the effect of the seepage on the boundary layer and on the immersed sediment weight could be parameterized in the form

$$\theta = \frac{u_{*o}^2\left(1-\alpha\frac{v}{u_{*0}}\right)}{gd_{50}\left(s-1-\beta\frac{v}{K}\right)} \tag{2}$$

where v=seepage velocity, positive upward and β=empirical parameter introduced to account for a possible reduction in the seepage force on the interfacial particles. Here, the denominator is similar to that proposed by Cheng and Chiew (1999) and the authors, but the potential effect of the seepage on modifying the boundary layer structure is also incorporated in the numerator.

If the porosity is correctly accounted for, then this equation should read

$$\theta = \frac{u_{*o}^2\left(1-\alpha\frac{v}{u_{*0}}\right)}{gd_{50}(s-1)\left(1-\beta\frac{v}{v_f}\right)} \tag{3}$$

where v_f=seepage velocity at incipient fluidization of the sediment bed. An alternative form is

$$\theta = \frac{u_{*o}^2\left(1-\alpha\frac{v}{u_{*0}}\right)}{gd_{50}(s-1)\left(1-\beta\frac{i}{i_c}\right)} \tag{4}$$

where the term in the denominator is equivalent to that proposed by Baldock and Holmes (1999) for $\beta=1$. Analogous results apply for the critical Shields parameter. Eqs. (3) and (4) correctly reduce the effective weight of the grains within the bed to zero for fluidized or piped conditions and reduce to the usual expressions for Shields number in the absence of seepage. Eq. (2) above and Eqs. (16) and (39) in the original paper do not yield zero effective stress within the bed for $i=\mathrm{i_c}=-v/K\approx-1$, which is the usual condition for incipient fluidization of sand beds (i.e., $s=2.65$, $n=0.4$).

Equations of the form of Eqs. (2)–(4), and equivalent equations in the original paper, which reduce the effective weight of the sediment, become unbounded as the denominator tends to zero, in physical terms as fluidization of the bed occurs (a state of zero effective stress). Consequently, using this modification of the Shields parameter, it is expected that for fluidized beds, incipient motion should occur at very low free stream flow rates and very large transport rates would occur under normal free stream flow conditions. However, this is contrary to both direct observation (Baldock and Holmes 1999), and can also be inferred from the data in the authors' paper. Their experiments show that the scour depths remain finite, even though the critical hydraulic gradient appears to be exceeded during their experiments for $Q_{seepage} > 140L/s$. Baldock and Holmes (1999) performed experiments with two different grain sizes and densities and both strong suction and injection, and observed no significant difference in the steady flow discharge required for incipient motion, consistent with much of previous experimental data cited above. Furthermore, incipient motion occurred at the same steady flow conditions even if the bed was totally fluidized (i.e., quick conditions).

Baldock and Holmes (1999) suggested that an explanation for this anomaly could be found by comparing the settling velocity, w_s, of the sediment particles with the velocity of the flow across the fluid/sediment interface, v. For a sand bed prior to fluidization, the maximum possible flow velocity out of the sand bed will be approximately equal to the hydraulic conductivity, K, assuming $i_c \approx -1 = -v/K$. This flow velocity is generally two orders of magnitude smaller than the settling velocity, w_s. However, once a particle lifts out of its bed recess and starts moving, it no longer experiences the seepage force that only acts *within* the bed matrix. Consequently, the self-weight, as paramterized by the settling velocity, dominates over the drag force from the small vertical flow out of the bed. The pressure gradient within the clear fluid is negligible. Essentially, the problem is that the Shields parameter represents a force balance on grains outside of the fluid-sediment matrix, whereas the seepage force acts only within the fluid-sediment matrix.

We therefore propose that the present treatment of this problem by equations of the form of Eq. (39) in the authors' paper or Eqs. (2)–(4) in the present paper is neither particularly convincing with regards the extensive experimental data, nor easily justified on the basis of the fluid physics. Nevertheless, seepage does affect the boundary layer at the very least through the injection or removal of fluid mass with different momentum and turbulence characteristics. This may lead to strong indirect effects on sediment transport through changes to suspended sediment concentration profiles or changes in bed forms.

The importance of the authors' paper is that it shows that it is critical to consider secondary effects on the sediment transport rates, and this may explain conflicting data from previous experimental studies, and should be carefully considered in future experiments. A secondary effect identified by Baldock and Holmes (1999) was that injection promoted ripple formation and changed ripple growth rates on an initially plane bed, while suction reduced ripple formation and indeed could prevent ripple formation entirely at low flow rates, even though particles continued to move as bed load. Baldock and Holmes (1999) found that changes in ripple regime led to significant changes in roughness and net suspended sediment transport. It would be instructive to know if the authors observed any changes in ripple size or ripple regime over the seepage box in their experiments.

Finally, Baldock and Holmes (1999) suggested that while seepage has little direct influence on saltating bed load particles, it might have a strong influence on sheet flow layers, since the layer may act as a fluid-sediment matrix within which the seepage force can act. Settling velocities are also reduced at high sediment transport concentrations (Nielsen et al. 2002; Baldock et al. 2004), and thus the vertical seepage velocity becomes relatively larger when compared to the particle settling velocity. Such conditions occur during the uprush and backwash of wave run-up on beaches, as well as within sheet flows in channel flows.

References

Baldock, T. E., and Holmes, P. (1999). "Seepage effects on sediment transport by waves and currents." *Proc., 26th Int Conf Coastal Engineering*, Copenhagen, ASCE, Reston, Va., 3601–3614.

Baldock, T. E., Tomkins, M. R., Nielsen, P., and Hughes, M. G. (2004). "Settling velocity of sediments at high concentrations." *Coast. Eng.*, 51(1), 91–100.

Chen, X., and Chiew, Y. M. (2004). "Velocity distribution of turbulent open-channel flow with bed suction." *J. Hydraul. Eng.*, 140(92), 140–148.

Cheng, N. S., and Chiew, Y. M. (1999). "Incipient motion with seepage." *J. Hydraul. Res.*, 37(95), 665–681.

Conley, D. C., and Inman, D. L. (1992). "Field observations of the fluid-granular boundary layer flow under near breaking waves." *J. Geophys. Res.*, 97(*No* C6), 9631–9643.

Conley, D. C., and Inman, D. L. (1994). "Ventilated oscillatory boundary layers." *J. Fluid Mech.*, 273, 261–284.

Davis, G. A., Hanslow, D. J., Hibbert, K., and Nielsen P. (1993). "Gravity drainage: A new method of beach stabilisation through drainage of the watertable." *Proc., 23rd Int Conf Coastal Eng.*, ASCE, Reston, Va., 1129–1141.

Francalanci, S., Parker, G., and Solar, L. (2008). "Effect of seepage-induced non-hydrostatic pressure distribution on bed-load transport and bed morphodynamics." *J. Hydraul. Eng.*, 134(4), 378–389.

Kruijt, J. A. (1976). "On the influence of seepage on incipient motion and sand transport." *Report No. STF60 AT6046*, Tech, Univ., Trondheim, Norway.

Löfquist, K. E. B. (1975). "An effect of permeability on sand transport by waves." *Tech Memo 62*, U.S. Army Coastal Eng. Res. Center.

Martin, C. S. (1970). "Effect of a porous sand bed on incipient sediment motion." *Water Resour. Res.*, 6(4), 1162–1174.

Nielsen, P. (1998). "Coastal groundwater dynamics." *Coastal Dynamics '97*, ASCE, Reston, Va., 546–555.

Nielsen, P., Robert, S., Moeller-Christiansen, B., and Oliva, P. (2001). "Infiltration effects on sediment mobility under waves." *Coast. Eng.*, 42(2), 105–114.

Oh, T.-M., and Dean, R. G. (1995). "Effects of controlled water table on beach profile dynamics." *Proc., 24th ICCE*, ASCE, 2449–2459.

Oldenziel, D. M., and Brink, E. E. (1974). *J. Hydr. Div.*, 100(7), 935–949.

Smith, G. N. (1968). *Elements of soil mechanics*, BSP Professional Books, London.

Turcotte, D. L. (1960). "A sub-layer theory for fluid injection into incompressible turbulent boundary layer." *J. Aerosp. Sci.*, 27(9), 675–678.

Watters, G. Z., and Rao, M. (1971). "Hydrodynamic effect of seepage on bed particles." *J. Hydr. Div.*, 97(3), 421–439.

Willetts, B. B., and Drossos, M. E. (1975). *J. Hydr. Div.*, 101(12), 1477–1488.

Closure to "Effect of Seepage-Induced Nonhydrostatic Pressure Distribution on Bed-Load Transport and Bed Morphodynamics" by Simona Francalanci, Gary Parker, and Luca Solari

April 2009, Vol. 134, No. 4, pp. 378–389.
DOI: 10.1061/(ASCE)0733-9429(2008)134:4(378)

Simona Francalanci[1]; Gary Parker[2]; and Luca Solari[3]

[1]Postdoctoral Researcher, CERAFRI, Center of Research and Advanced Education for Hydrogeological Risk Prevention, Via XI Febbraio 2, 55040 Retignano di Stazzema (LU), Italy. E-mail: simona.francalanci@dicea.unifi.it

[2]Prof., Ven Te Chow Hydrosystems Laboratory, Univ. of Illinois, 205 N. Mathews Ave., Urbana, IL 61801. E-mail: parkerg@uiuc.edu

[3]Asst. Prof., Dept. of Civil and Environmental Engineering, Univ. di Firenze, Via S. Marta 3, 50139 Firenze, Italy. E-mail: luca.solari@dicea.unifi.it

The writers deeply appreciate this thoughtful discussion, which was also quite thought-provoking (see below). The discussers

offer an encyclopedic overview of research on the effect of seepage forces on sediment motion. The many papers they cite highlight the value of research in this area.

We begin by enumerating the ways in which our experiments differ from previous experimental work cited by the discussers. Martin (1970) considered incipient motion for the case of unidirectional pipe flow. The experiments of Baldock and Holmes (1999) include both the cases of unidirectional flow and wave motion with a free surface. In the case of unidirectional flow, however, only the condition of incipient motion was considered. The experiments of Cheng and Chiew (1999) likewise pertain only to incipient motion. Our experiments extend this work to the case of a fully mobile bed.

As far as we know, our experiments are the first to treat the effect of seepage on active sediment transport under sustained, unidirectional flow. The experiments were run for 12–16 h to establish mobile-bed equilibrium in the absence of a zone of seepage. After taking measurements, they were then continued for 2–4 h more to establish mobile-bed equilibrium in the presence of a zone of seepage. Measurements were taken both 10 min after the commencement of seepage and at mobile-bed equilibrium.

The results are unambiguous. In our experiments, upward seepage caused erosion in the seepage zone, ultimately resulting in a depression at mobile-bed equilibrium. Downward seepage caused deposition, ultimately resulting in an elevated zone at mobile-bed equilibrium. The scour can only have resulted from a tendency for enhanced sediment transport in the presence of upward seepage, and the fill can only have resulted from the opposite tendency in the presence of downward seepage. We believe that our data constitute a benchmark for testing theoretical frameworks of the type outlined in our paper and the two papers cited by the discussers, Nielsen (1998) and Baldock and Holmes (1999).

Having said this, we recognize that the discussers have detected an inconsistency in our own theoretical treatment. Specifically, the formulation leading to Eq. (16) of our paper is inconsistent with the formulation leading to Eq. (32) of the same paper. The writers accept the discussers' contention that the physical basis for the latter formulation, which is due to Cheng and Chiew (1999), is the correct one.

In the context of the analysis presented in our paper, the corrected form is

$$\tau_* = \frac{\tau_b}{\left\{\rho_s - \rho\left[1 + \frac{v_s}{K(1-\lambda_p)}\right]\right\} gD} \tag{1}$$

The discussers point out that they and their coauthors have previously proposed forms similar to Eq. (1). Specifically, Nielsen (1998) proposed a form [Eq. (9) therein] which in the present notation takes the form

$$\tau_* = \frac{\tau_b}{\left[\rho_s - \rho\left(1 + \beta\frac{v_s}{K}\right)\right] gD} \tag{2}$$

The parameter β, which Nielsen (1998) approximated as 0.5, is intended to account for a possible suppression in the seepage force on particles exposed at the bed. Baldock and Holmes (1999) have proposed a form [Eq. (5) therein] which is identical to Eq. (1) above. These papers should have been cited in our paper. The writers acknowledge a lack of diligence in failing to track them down in the relevant conference proceedings.

The form of the modified Shields number proposed by Nielsen (1998) evidently contains the same error as that of Eq. (16) of our paper. The discussers, however, usefully incorporate the suppression coefficient β into a modified form of Eq. (1)

$$\tau_* = \frac{\tau_b}{\left\{\rho_s - \rho\left[1 + \frac{\beta v_s}{K(1-\lambda_p)}\right]\right\} gD} \tag{3}$$

The above equation corresponds to Eq. (4) of the discussers'. Using the porosity $\lambda_p = 0.30$ pertaining to the experiments of our paper and a value of β of 1 (Baldock and Holmes 1999), Eq. (3) indicates that the term v_s/K of our Eq. (16) should be corrected to $1.43\ v_s/K$. Using the same value of λ_p and a value of β of 0.5 [as suggested by Nielsen (1998) based on Martin (1970)], the term v_s/K should be corrected to $0.71\ v_s/K$, while a value of β of 0.7 would correspond to no correction. Thus while the derivation of Eq. (16) of our paper does indeed contain a nontrivial error which we hereby correct, the numerical predictions using such equation appear to be within the range of uncertainty suggested by the discussers.

We have used the example of Runs 1–3 (upward seepage) of our paper to test the effect of amending Eq. (16) of our paper to Eq. (3) in the numerical model. We know that the value $\beta = 0.7$ recovers our original analysis. With this in mind, we have performed numerical runs with $\beta = 0.5$ and 1.0 as well. Fig. 1 shows

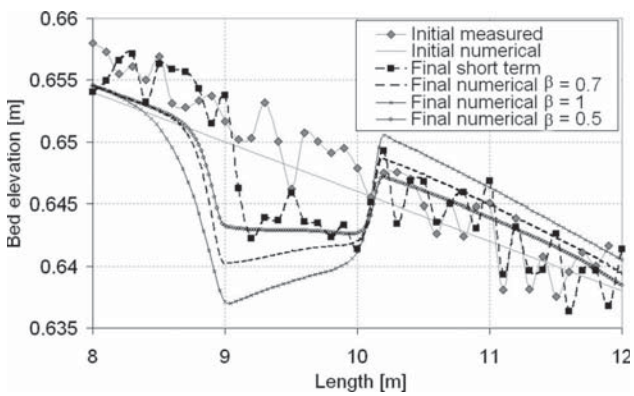

Fig. 1. Comparison of experimental and numerical results, Runs 1–3: short-term experiment

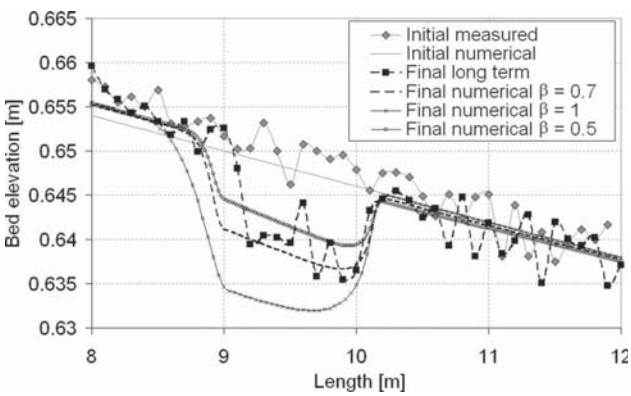

Fig. 2. Comparison of experimental and numerical results, Runs 1–3: long-term experiment

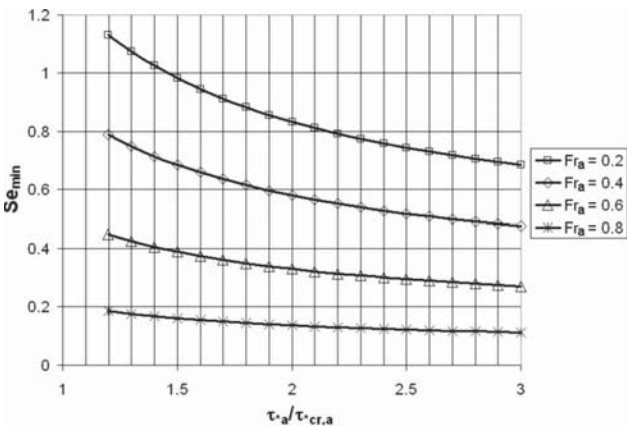

Fig. 3. Se_{min} as a function of $\tau_{*a}/\tau_{*cr,a}$ (Fr_a=0.2, 0.4, 0.6 and 0.8)

the results of these numerical runs, along with the data for the short-term experiment. Fig. 2 shows the corresponding plot for the long-term experiment. The numerical results for the case $\beta = 1.0$ somewhat overpredict the tendency for scour in the presence of upward seepage, suggesting the adoption of a value higher than 0.5 but lower than 1.0. The numerical runs with all three values of β, however, agree with the sense of the data; upward seepage produced enhanced sediment transport, resulting in scour.

The delineation of Eq. (3) should properly be considered the achievement of Nielsen (1998) and Baldock and Holmes (1999). Here we attempt to counter their pessimism concerning the structure of their own (and our) formulations, as expressed in the following quote. "We therefore propose that the present treatment of this problem by [such equation] is neither particularly convincing with regards the extensive experimental data, nor easily justified on the basis of the fluid physics."

The pessimism of the discussers seems to derive from two considerations: (1) the observation that the available data display disparate tendencies which may not be easily captured with frameworks that use relations of the type of Eq. (3); and (2) doubts concerning whether or not seepage forces affect the dynamics of particles participating in bed-load transport.

We begin by considering the second consideration mentioned. The discussers state, with regard to the threshold of motion, the following: "Baldock and Holmes (1999) performed experiments with . . . both strong suction and injection, and observed no significant difference in the steady flow discharge required for incipient motion, consistent with much of previous experimental data cited above." We believe that Cheng and Chiew (1999) have provided a physically justifiable theory of incipient motion in the presence of seepage effects, and have justified it extensively via experiments. It is their formulation that we have used in our framework. We believe that we are on solid ground here.

Also in regard to consideration two, the discussers state as follows: "once a particle lifts out of its bed recess and starts moving, it no longer experiences the seepage force that only acts within the bed matrix." The implication is that seepage forces should not significantly affect bed-load transport itself. We offer the following counterargument. The volume bed-load transport rate per unit width q_b can be expressed as

$$q_b = E_b L_{step} \tag{4}$$

where E_b denotes the volume rate of entrainment of bed particles into bed-load per unit area and L_{step} denotes the average step length of a particle. Extensive research has shown that while E_b varies strongly with Shields number, L_{step} shows a much weaker dependence (Fernández Luque and van Beek 1976; Wong et al. 2007). Entrainment of a bed particle is a function of the forces at the bed, not after it has begun motion. With this in mind, we expect that seepage should enter into the physics of bed-load transport via the parameter E_b.

It may be that the effect of seepage on the parameter τ_* characterizing the Shields number of particles participating in motion is somewhat reduced compared to its effect on τ_{*cr}. Such a tendency may indeed be reflected in Figs. 1 and 2. That is, in the simulation using the suppression factor $\beta = 0.7$ (which recovers our original calculation and fits the data well) in Eq. (3) for τ_*, we have not used a similar suppression factor τ_{*cr} in the relation for the threshold of motion of Cheng and Chiew (1999), instead using their original relation.

Before proceeding to consideration one, we elaborate on the following statement of the discussers: "The authors ignore the possible influence of the seepage in directly modifying the bed shear stress in their model. However, very importantly, they include the continuity effect." We believe the two formulations amount to (more or less) the same thing, so that the incorporation of both would be double bookkeeping. Cheng and Chiew (1998a) offer a formulation of the type suggested by the discussers, Cheng and Chiew (1998b) offer the same formulation used in our paper, and Cheng and Chiew (1999, p. 674) indicate that the two methods show good agreement.

We now proceed to consideration one, the fact that disparate results obtained to date cast doubts on formulations of the type in our paper. The constructive comments of the discussers motivated us to address the issue of disparate results. In doing this we use precisely the framework presented in our paper, with the exceptions that (1) Eq. (3) is used instead of the corresponding form in that paper, and (2) form drag is neglected in the bed-load transport equation. We return to the issue of form drag and bed forms below.

The bed-load transport is evaluated with Eq. (24) of our paper, neglecting form drag. This relation indicates that sediment mobility in the presence of seepage is enhanced if seepage increases the excess Shields number above the critical value, and vice versa. Linearized perturbation analysis of our framework in the limit of small v_s, applied to a bed that has not yet had time to respond morphodynamically to seepage, allows us to estimate conditions for enhanced bed mobility (mediated by dominant buoyancy effects) versus suppressed mobility (mediated by dominant suppression of bed shear stress).

Our results are encapsulated in terms of a dimensionless parameter, which we term the seepage number, defined as follows

$$\mathbf{Se} = \frac{KL}{U_a H_a} \tag{5}$$

In the above relation and subsequent relations, the subscript "a" refers to antecedent conditions in the absence of seepage.

For the sake of clarity we focus on upward seepage. The main result can be summarized as follows. When $\mathbf{Se} < \mathbf{Se}_{min}$, where $\mathbf{Se}_{min}$ is an order one quantity, buoyancy effects dominate, and mobility is enhanced everywhere in the seepage zone. As $\mathbf{Se} > \mathbf{Se}_{min}$, a subzone of suppressed mobility due to bed shear stress reduction appears from the upstream end of the seepage zone. This subzone extends downstream as **Se** increases, eventually reaching a value of at least (7/10)L. The relation for $\mathbf{Se}_{min}$ is as follows:

$$\mathbf{Se}_{\min} = \frac{KL_{\min}}{U_a H_a} = \frac{(M_1\beta + M_2 R)}{RM_1(1-\lambda_p)\left(\frac{7}{3}X - \frac{14}{15}\right)} \tag{6}$$

where

$$X = \frac{1+\mathbf{Fr}_a^2}{1-\mathbf{Fr}_a^2} \tag{7a}$$

$$M_1 = \frac{\tau_{*a}}{\tau_{*a} - \tau_{*cr,a}}, \tag{7b}$$

$$M_2 = \frac{\tau_{*cr,a}}{\tau_{*a} - \tau_{*cr,a}} \tag{7c}$$

$$R = \frac{\rho_s}{\rho} - 1 \tag{7d}$$

and $\mathbf{Fr}_a$ denotes the Froude number of the ambient flow. Computations indicate that in general $\mathbf{Se}_{\min}$ is an order-one parameter. Fig. 3 shows a plot of $\mathbf{Se}_{\min}$ as a function of $\tau_{*a}/\tau_{*cr,a}$ for the values $\mathbf{Fr}_a$=0.2, 0.4, 0.6 and 0.8. In the plots, it has been assumed that R=1.65 (quartz), β=0.7 and λ_p=0.3; that is, values applying to our experiments.

This analysis can explain conditions under which upward seepage results in either enhanced or suppressed mobility. We checked the above analysis against all 29 of our own experiments pertaining to ambient conditions (no seepage). In these experiments, $\mathbf{Fr}_a$ ranged from 0.61 to 0.74. Values of **Se** computed for our experiments ranged from 0.08 to 0.171; values of $\mathbf{Se}_{\min}$ computed with Eq. (6) ranged from 0.14 to 0.27. In all 29 cases $\mathbf{Se}/\mathbf{Se}_{\min}$ was less than unity. That is, our theory applied at the linear level indicates that upward seepage would cause enhanced mobility, as we observed.

Our computed values of $\mathbf{Se}/\mathbf{Se}_{\min}$ ranged from 0.52 to 0.79. If $\mathbf{Se}/\mathbf{Se}_{\min} > 1$, Eq. (6) indicates that a subzone would appear within which mobility would be suppressed rather than enhanced by upward seepage. For sufficiently large values of $\mathbf{Se}/\mathbf{Se}_{\min}$, mobility suppression would dominate over the greater portion of the zone of seepage. According to Eq. (6), this could have been achieved by e.g., increasing the length of the zone of seepage L or the hydraulic conductivity K.

To summarize, the same theoretical framework can explain disparate tendencies. It may turn out that this framework remains incomplete, but we are more optimistic than the discussers in thinking that it offers a roadmap for future research.

A final point concerns bedforms. As can be seen from Figs. 3 and 4 of our paper, the bedforms were of low amplitude, and their form drag never contributed more that 20% of the bed resistance. Detailed bed profiles were taken during the experiments (Francalanci 2006); these did not indicate that seepage had a major effect on them. We feel it unlikely that the presence of bedforms is the cause of the enhanced/suppressed mobility induced by upward/downward seepage. This point, however, merits verification by means of experiments under conditions of lower-regime plane-bed.

We thank the discussers for their highly stimulating observations. We also thank Yee-Meng Chiew, who greatly helped us in our thinking about the reasons for disparate results.

References

Baldock, T. E., and Holmes, P. (1999). "Seepage effects on sediment transport by waves and currents." *Proc., 26th Int. Conf. on Coastal Engineering*, ASCE, Reston, Va., 3601–3614.

Cheng, N. S., and Chiew, Y. M. (1998a). "Modified logarithmic law for velocity distribution subjected to upward seepage." *J. Hydraul. Eng.*, 124(12), 1235–1241.

Cheng, N. S., and Chiew, Y. M. (1998b). "Turbulent open-channel flow with upward seepage." *J. Hydraul. Res.*, 36(3), 415–431.

Cheng, N. S., and Chiew, Y. M. (1999). "Incipient sediment motion with seepage." *J. Hydraul. Res.*, 37(5), 665–681.

Fernández Luque, R., and van Beek, R. (1976). "Erosion and transport of bed-load sediment." *J. Hydraul. Res.*, 14(2), 127–144.

Francalanci, S. (2006). "Sediment transport processes and local scale effects on river morphodynamics." Ph.D. thesis, Univ. of Padova, Padova, Italy.

Martin, C. S. (1970). "Effect of a porous sand bed on incipient sediment motion." *Water Resour. Res.*, 6(4), 1162–1174.

Nielsen, P. (1998). "Coastal groundwater dynamics." *Coastal dynamics '97*, ASCE, Reston, Va., 546–555.

Wong, M., Parker, G., De Vries, P., Brown, T., and Burges, S. J. (2007). "Experiments on dispersion of tracer stones under lower-regime plane-bed equilibrium bed load transport." *Water Resources Research*, 43(3), W03440.

Discussion of "Coherent Structures in the Flow Field around a Circular Cylinder with Scour Hole" by G. Kirkil, S. G. Constaninescu, and R. Ettema

May 2008, Vol. 134, No. 5, pp. 572–587.
DOI: 10.1061/(ASCE)0733–9429(2008)134:5(572)

Christian Gobert[1]; Oscar Link[2]; Michael Manhart[3]; and Ulrich Zanke[4]

[1]Ph.D. Candidate, Fachgebiet Hydromechanik, Technische Universität München, Arcisstr. 21, 80333 München, Germany. E-mail: ch.gobert@bv.tum.de

[2]Asst. Prof., Dept. of Civil Engineering, Univ. of Concepción, Edmundo Larenas 270, Concepción, Chile. E-mail: olink@udec.cl

[3]Prof., Fachgebiet Hydromechanik, Technische Universität München, Arcisstr. 21, 80333 München, Germany. E-mail: m.manhart@bv.tum.de

[4]Prof., Institute for Hydraulic and Water Resources Engineering, Darmstadt Univ. of Technology, Rundeturmstraße 1, 64283. Germany. E-mail: wabau@wb.tu-darmstadt.de

Kirkil et al. (2008) are complimented on their study involving both laboratory experiment and large eddy simulation (LES), which contribute significantly to the understanding of scour mechanisms around a bridge pier. Recently, the discussers studied the interaction between flow field and sediment bed at a circular cylinder in sand by similar experiments and obtained comparable results that serve to extend the authors' conclusions.

The authors presented laboratory-flume visualizations and results of LES to investigate coherent structures present in the flow field around a circular cylinder located in an equilibrium scour hole in sand. By a remarkable analysis of the flow in the scour hole, they found a system of vortices (horseshoe vortex system, HV) more complex than hitherto indicated in literature.

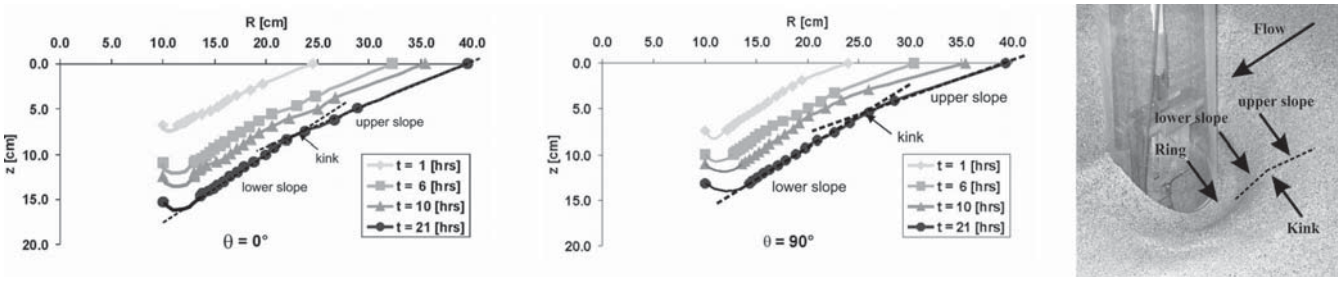

Fig. 1. Left and center: developing scour holes on the azimuthal half-planes with θ=0° and θ=90°. Right: photo of the scour hole

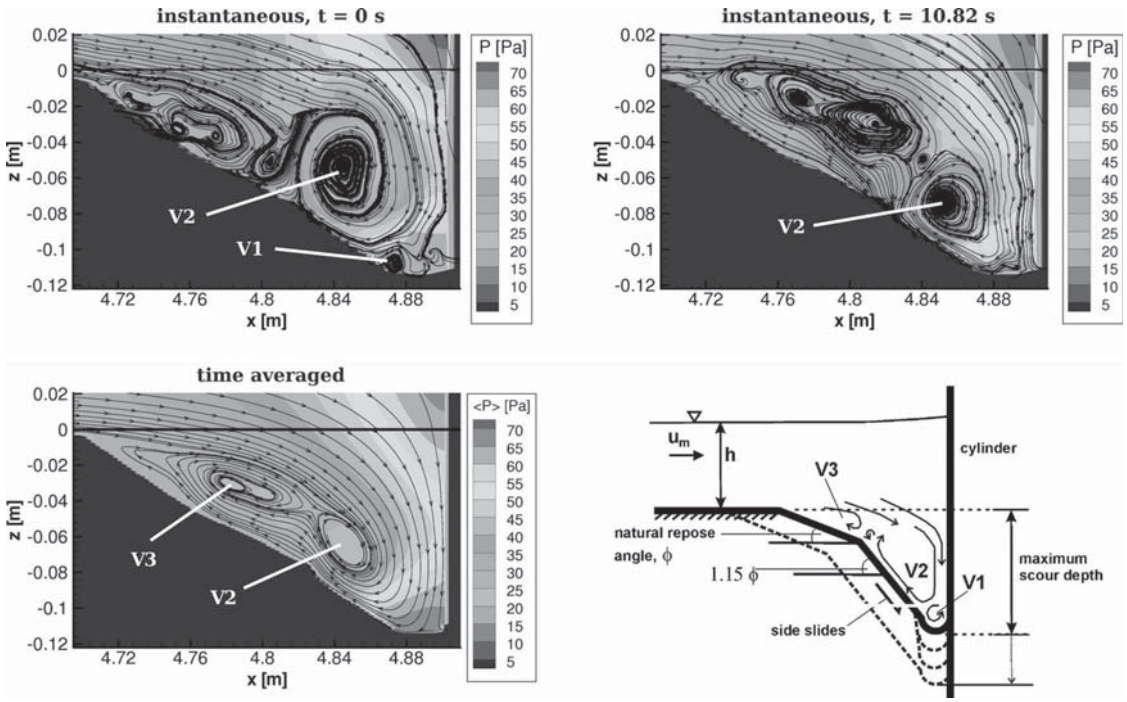

Fig. 2. Streamlines and pressure at θ=0° from instantaneous and time averaged fields. Bottom right: schematic of the scour mechanism in sand.

In the discussers' work bathymetry and flow at slightly different conditions than those of the authors were investigated. The Reynolds number based on bulk velocity and flow depth was Re_b=90,000, five times larger than in the authors' work, based on pier diameter it was Re_p=60,000. The critical friction velocity ratio was 0.95. The sand bed grain sizes ranged between 0.6 and 2.0 mm, with a mean diameter of 0.97 mm. For the simulations, the discussers discretized the flow with up to 213 Mio. control volumes. For further details on the discussers' laboratory and numerical experiments please refer to Link (2006) and Link et al. (2008a, b).

In the present discussion, the discussers highlight three points on the interaction between the HV and the scour-hole geometry that were not treated by the authors. These concern (1) bathymetry; (2) layout and dynamics of the HV; and (3) effects of time averaging.

Bathymetry

The discussers observed a similar final bathymetry as depicted in the authors' Figs. 3, 4, and 6. In Fig. 1 are plotted profiles of the sediment bed after 1, 6, 10, and 21 h on azimuthal half-planes with θ=0 and 90°. Three regions can be distinguished: a ring-shaped portion close to the cylinder base, a steep slope in the deeper part of the scour hole, and a mild slope in the upper part of it. Both slopes are separated by a clearly distinguishable kink in the bed (Fig. 1). The shape of the scour hole remained nearly constant during scour development. Below the kink, the slope of the bed was measured to be 42°, while above the kink, the slope was 29°. The overall average slope was 35.5°, which is about 15% higher than the natural repose angle of the sand (30°). The observed scour-slopes suggest that the HV consist of at least three vortices of different intensities.

Layout and Dynamics of HV

Fig. 2 shows instantaneous fields from the discussers' numerical experiment, similar to the authors' Fig. 4. Three to four vortices can be distinguished. As indicated in the figure, two vortices V1 and V2 are found close to the pier. From animations the discussers found that the most stable vortex is V2. This vortex is trapped

in the scour hole and is observed at almost every instant whereas V1 cannot always be observed. Upstream of V2, a complex pattern of strongly intermittent vortices can be found. In comparison, the authors found three stable vortices in the scour hole. Taking into consideration that in the authors' work the Reynolds number is smaller than in the discussers' work, it can be concluded that frequency of vortex shedding and intermittency of vortices increases with Reynolds number.

Effects of Time Averaging

The discussers have also investigated differences between instantaneous and time-averaged flow fields. This is of practical relevance since for cases in which time-averaged fields provide meaningful results, Reynolds averaged simulations (RANS) with appropriate closure models are a computationally less expensive alternative to LES for flow analysis. The authors found that the time-averaged flow field shows a similar vortex system as instantaneous flow. In contrast, the discussers observed in the averaged and instantaneous fields two and up to four vortices respectively (Fig. 2). This provides evidence that the leftmost vortex is not stable. One might conclude that this vortex is only an artifact of averaging because the instantaneous fields showed that in this region frequent vortex shedding and detachment takes place, a process that is hidden by time averaging. Thus, depending on the actual configuration, results from RANS might be misleading.

The discussers conclude that shedding, dissipation, and interaction of vortices in the scour hole depends on the Reynolds number. Averaged flow fields and the corresponding bed shear stresses alone are not able to completely explain the scour mechanism at a cylinder. Based on the discussers' observations and those of the authors, the discussers schematically depicted the scour mechanism in Fig. 2 (bottom right). Close to the cylinder, scouring is controlled by the vortex V1, which appears only intermittently. Farther upstream, a very stable counterrotating vortex V2 is observed. V2 rotates such that the flow near the bed points upstream whereas the flow near the bed below V1 points downstream. This explains the shape of the bed in these sections: at V1, the bed is flat because V1 transports sediment downstream, whereas at V2 the inclination of the bed is higher than the repose angle because V2 transports upstream and stabilizes the slope. At instances when V2 weakens, sediment slides down and is fed into V1.

Acknowledgments

Financial support of the Chilean Research Council, CONICYT, through grant 11080126 is acknowledged.

References

Kirkil, G., Constantinescu, S., and Ettema, R. (2008). "Coherent structures in the flow field around a circular cylinder with scour hole." *J. Hydraul. Eng.*, 134(5), 572–587.

Link, O. (2006). "An investigation on scouring around a single cylindrical pier in sand." Mitteilungen des Institutes für Wasserbau und Wasserwirtschaft der Technischen Universität Darmstadt, Nr. 136 (in German).

Link, O., Gobert, Ch., Manhart, M., and Zanke, U. (2008a). "Effect of the horseshoe vortex system on the geometry of a developing scour hole at a cylinder." *Proc. 4th Int. Conf. on Scour and Erosion*.

Link, O., Pfleger, F., and Zanke, U. (2008b). "Characteristics of developing scour-holes at a sand-embedded cylinder." *Int. J. Sediment Res.*, 23, 268–276.

Closure to "Coherent Structures in the Flow Field around a Circular Cylinder with Scour Hole" by G. Kirkil, S. G. Constantinescu, and R. Ettema

May 2008, Vol. 134, No. 5, pp.572–587.
DOI: 10.1061/(ASCE)0733-9429(2009)134:5(572)

G. Kirkil, M.ASCE[1]; S. G. Constantinescu, M.ASCE[2]; and R. Ettema, M.ASCE[3]

[1]Graduate Research Asst., Civil & Environmental Engineering Dept., IIHR-Hydroscience and Engineering, The Univ. of Iowa, Stanley Hydraulics Laboratory, Iowa City, IA 52242; currently, Postdoctoral Research Staff Member, Atmospheric, Earth and Energy Division, Lawrence Livermore National Lab, P.O. Box 808, L-103, Livermore, CA 94551. E-mail: gokhan-kirkil@uiowa.edu; kirkil1@llnl.gov

[2]Assoc. Prof., Civil & Environmental Engineering, IIHR-Hydroscience and Engineering, The Univ. of Iowa, Stanley Hydraulics Laboratory, Iowa City, IA 52242. E-mail: sconstan@engineering.uiowa.edu

[3]Prof., College of Engineering and Applied Science, The Univ. of Wyoming, Laramie, WY 82071. E-mail: rettema@uwyo.edu

The writers wish to thank the discussers for their kind words and comments. The discussers are commended for bringing out interesting issues in relation to large eddy simulation (LES) of flow and turbulence structure at circular cylinders in loose bed channels, in particular related to the effects of Reynolds number and bathymetry shape. We think the fact that the main features of the flow fields are to a large degree similar in two LES investigations conducted with different numerical codes gives additional confidence in the approach chosen by the writers and the discussers. Several specific comments of the discussers are addressed below. Our comments are also based on additional results (see Kirkil, Constantinescu, and Ettema 2009b; Kirkil and Constantinescu 2009a; Koken and Constantinescu 2009) obtained by our group using detached eddy simulation (DES). In particular, the DES simulation of Kirkil, Constantinescu, and Ettema (2009b) was performed at a cylinder Reynolds number of $2.06*10^5$. The DES simulation further extends the range of Reynolds numbers needed to understand and quantify scale effects on the flow and turbulence structure. The Reynolds number of the numerical investigation conducted by the discussers falls in between ($Re_D=60{,}000$, D is the cylinder diameter).

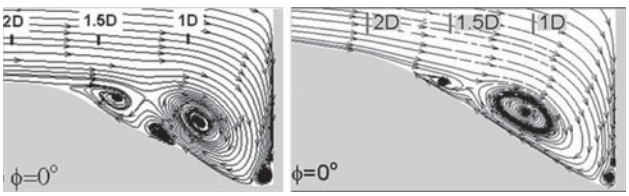

Fig. 1. Mean flow streamlines in the $\phi=0°$ plane a) $Re_D=16{,}000$; (b) $Re_D=2.06*10^5$

The change in the bed slope within the scour hole observed by the discussers was documented by several experiments (Unger and Hager 2007). The difference between the two slopes tends to decrease as the bed evolves toward equilibrium. In our experiments, including in the ones performed at $Re_D = 2.06 * 10^5$, the change in the bed slope within the scour hole was found to be relatively small. Despite this, the mean flow topology at $Re_D = 16{,}000$ and $Re_D = 2.06 * 10^5$ as visualized by 2D streamlines (Fig. 1) was found to be similar within the scour hole, especially near the symmetry plane (polar angle $\phi = 0°$), and to contain two main necklace vortices that can be associated with V2 and V3 in the mean flow results presented by the discussers (Fig. 2 of the discussion).

We fully agree with the conclusion by the discussers that the vortical system inside the scour hole consists of at least three vortices of different intensities (two main necklace vortices, one junction vortex and, depending on the bathymetry and other flow conditions, a number of bottom wall-attached vortices induced by the presence of the main necklace vortices). A difference observed in the mean flow patterns in the symmetry plane between the simulations performed by the authors and the discussers is the presence in our simulation at $Re_D = 16{,}000$ of a bottom-attached vortex between the main two necklace vortices and especially of a small, but strongly coherent, junction vortex at the base of the cylinder at both Reynolds numbers. Though the differences in the flow conditions and bathymetry explain the absence of the bottom-attached vortex in the mean flow patterns predicted in the simulation conducted by the discussers and in our simulation at $Re_D = 2.06 * 10^5$ [Fig. 1(b)], the absence of a well-defined junction vortex is more surprising, given the fact that experiments have always shown the formation of that vortex, which is in fact responsible for the slight increase of the bathymetry levels very close to the cylinder. Though a small vortex denoted V1 is observed in the instantaneous flow fields predicted by the discussers (Fig. 2 in the discussion), that vortex is in fact a bottom-attached vortex induced by the main necklace vortex V2 rather than a true junction vortex as shown in the sketch in the same figure. In the simulation performed by the discussers a junction vortex is not present in the mean flow field in the $\phi = 0°$ plane despite the presence of a well-defined downflow with streamlines deflected toward the cylinder as the bed is approached. The fact that in the instantaneous flow the 2D streamlines close to the cylinder are not always tangent to the cylinder surface suggests a problem related to the resolution of the flow in that region. Comparison of our simulations at $Re_D = 16{,}000$ and $Re_D = 2.06 * 10^5$ (for more details, see Kirkil, Constantinescu, and Ettema 2009b) shows that a main scale effect is the reduction of the lateral extent of the upstream necklace vortex V3 with the increase in the Reynolds number. For example, that vortex is still present in the $\phi = 45°$ section at $Re_D = 16{,}000$ but absent for $|\phi| > 30°$ in the $Re_D = 2.06 * 10^5$ simulation.

Related to the unsteady dynamics of the necklace vortices, our results at both Reynolds numbers are fully consistent with those by the discussers in the sense that the vortex denoted V2 in their discussion (main necklace vortex in our paper) is the most coherent and stable vortex while, at times, the coherence of the main secondary vortex V3 is lost and the region is populated by a large number of smaller eddies. In fact, the instantaneous flow structure visualized in Fig. 4 of our paper is fully consistent with this scenario. One important point, already mentioned in the original article is that the presence of a certain number of vortices in the mean flow does not necessarily mean that they have a direct correspondent in the instantaneous flow fields or that they are stable, in the sense that they can be recognized in each of the instantaneous flow fields. As the discussers correctly point out, that is the case for V2 and, based on our results, for the junction vortex but not for the primary secondary vortex V3 or for the small vortices shed from the separating region of the incoming boundary layer. We do not think V3 is an artifact of the averaging. This is because such a vortex is present at small polar angles over more than 50% of the time in our simulations. However, depending on the shape of the scour hole, this is a distinct possibility especially during the initial stages of the development of the scour hole. In this regard, the comment by the discussers that results from RANS might be misleading to understand the structure of the HV system in the instantaneous flow fields is a very important one. For example, a similar problem arises when the structure of the detached shear layers on the sides of the cylinder is analyzed based on RANS or even unsteady RANS results. Unsteady RANS simulations do not capture the vortex tubes shed in the separated shear layers, which play a determinant role in determining the turbulence structure of the near wake region despite capturing the large-scale shedding of the rollers.

We do not think comparison of Figs. 4 and 6 in our paper suggests the time-averaged flow fields show a similar vortex system as the instantaneous flow at $Re_D = 16{,}000$. In fact, we fully agree with the discussers that is not the case in the region between the separation line of the incoming boundary layer and the main necklace vortex V2. Animations of the instantaneous flow patterns from the solutions obtained by the authors support that observation at both Reynolds numbers. We also agree that the Reynolds number has an influence on the dynamics of the horseshoe vortex system inside the scour hole. However, comparison of the LES and DES simulations (Kirkil, Constantinescu, and Ettema 2009b) performed by the writers clearly shows that the main necklace vortex is subject to bimodal oscillations at both Reynolds numbers. The large-scale bimodal oscillations of this necklace vortex are the main reason for the large amplification of the turbulence within the scour hole in front of the cylinder. Another very relevant result related to scale effects is that the increase in the Reynolds number decreases the amplitude of the bimodal oscillation of the main necklace vortex V2. The discussers' comment that the intermittency of the vortices increases with the Reynolds number is consistent with our DES results.

We fundamentally agree with the discussion of the scour mechanism by the discussers. We have two comments based on our LES and DES results. The first is that in our simulations the junction vortex is quite stable and strong, consistent with most experimental investigations. Still, large-scale temporal variations in its strength are observed, especially during the times the main necklace vortex approaches the face of the cylinder or a large eddy is convected with the downflow parallel to the face of the cylinder. We would also like to point out that the formation of a horseshoe vortex system containing two main necklace vortices (V2 and V3 in the notation used by the discussers) does not necessarily imply the bathymetry inside the upstream part of the scour hole should display a large change in the bed slope in between the two vortices.

References

Kirkil, G., and Constantinescu, G. (2009a). "Nature of flow and turbulence structure around an in-stream vertical plate in a shallow channel and the implications for sediment erosion." *Water Resour. Res.*, 44, W06412.

Kirkil, G., Constantinescu, G., and Ettema, R. (2009b). "DES investigation of turbulence and sediment transport at a circular pier with scour

hole." *J. Hydraul. Eng.*, 135(11), 888–901.
Koken, M., and Constantinescu, G. (2009). "An investigation of the dynamics of coherent structures in a turbulent channel flow with a vertical sidewall obstruction." *Phys. Fluids*, 21, 085104.
Unger, J., and Hager, W. H. (2007). "Downflow and horseshoe vortex characteristics of sediment embedded bridge piers." *Exp. Fluids*, 42(1), 1–19.

Discussion of "Inception Point and Air Concentration in Flows on Stepped Chutes Lined with Wedge-Shaped Concrete Blocks" by Antònio T. Relvas and Antònio N. Pinheiro

August 2008, Vol. 134, No. 8, pp. 1042–1051.
DOI: 10.1061/(ASCE)0733-9429(2008)134:8(1042)

Sanjay W. Thakare[1] and Sandip P. Tatewar[2]
[1]Lecturer, Dept. of Civil Engineering, Government College of Engineering, Amravati. 444 604, India. E-mail: thakare.sanjay@gcoea.ac.in
[2]Asst. Prof., Dept. of Civil Engineering, Government College of Engineering, Amravati, 444 604, India. E-mail: sandiptatewar@yahoo.co.in

The authors are to be congratulated for carrying out a systematic investigation of flow over a stepped chute lined with wedge-shaped concrete blocks (hereafter called a stepped block spillway). As mentioned by the authors, Pinheiro and Revels (2000) showed that the channel excavated in the embankment and protected with wedge-shaped precast concrete blocks can offer an inexpensive alternative to conventional concrete-cast in-situ solutions. The discussers carried out a case study of Chandrabhaga River Project in the Maharashtra State of India, for which a conventional ogee spillway is provided. Thakare et al. (2008) designed a stepped block spillway following CIRIA design guidelines (Hewlett et al. 1997). In this project, it was found that the cost required for a stepped block spillway was considerably less than that of the existing ogee spillway. The stepped block spillway has, therefore, considerable potential as a low cost method for providing a spillway and the protection of embankment from erosion by overtopping flow. Hence, the discussers support the authors' statement that stepped-block spillways are a promising solution to provide overtopping protection for embankment dam if the discharge capacity of the existing spillway is not adequate.

Stepped-block spillways are generally associated with embankment dams for overtopping protection and hence designed for flatter slopes ($h_s/l_s=0.25$ to 0.50), whereas stepped spillways are generally associated with concrete dams and designed for steeper slopes ($h_s/l_s=1.25$ to 1.66). Fig. 1 shows that the difference between the values of h_c/h_s predicted by equations [Chanson (1996) and Andre (2004)] and experimental values for gabion-stepped spillway is large for flatter slopes as compared to that for steeper slopes. The authors compared the characteristics of flow (like onset of skimming flow, location of inception point, and air concentration) over a stepped-block spillway with those of a stepped spillway for roller compacted concrete dams. In the latter case, the steps are impervious, whereas a stepped-block spillway allows the percolation of flow through the joints between the blocks. A gabion-stepped spillway also permits infiltration of flow inside the rocks, which is similar in nature to the flow over stepped block spillway. This infiltration modifies the characteris-

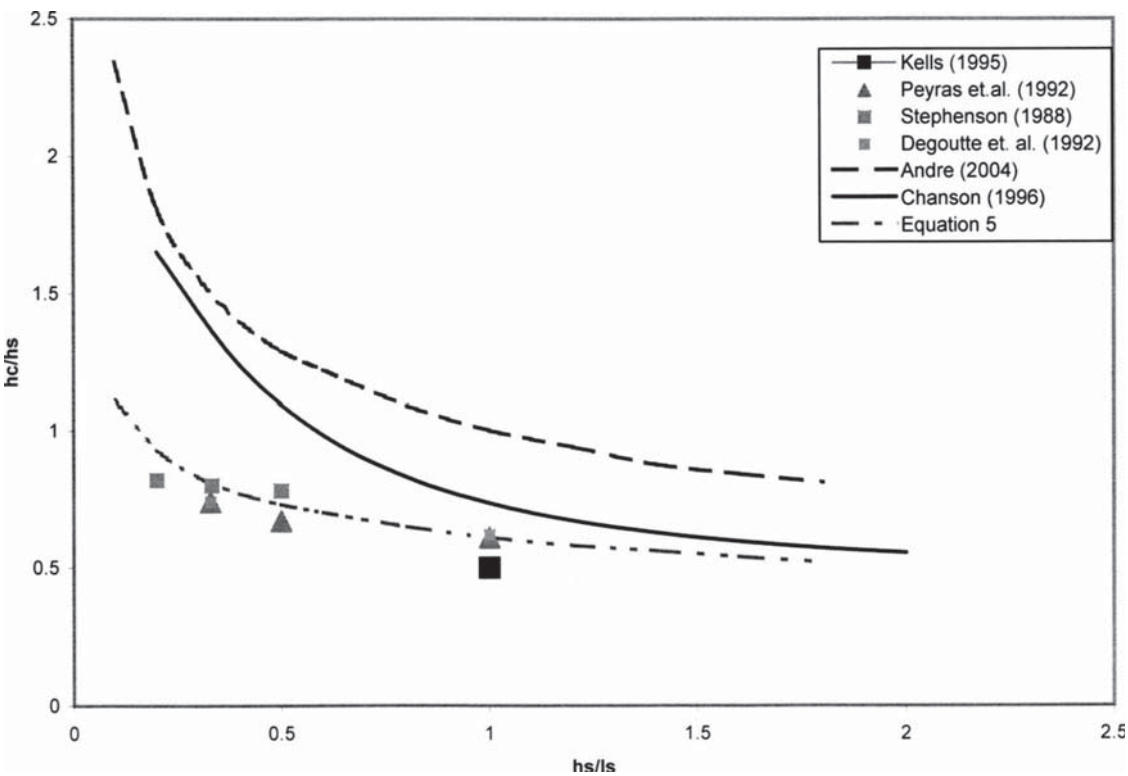

Fig. 1. Onset of skimming flow

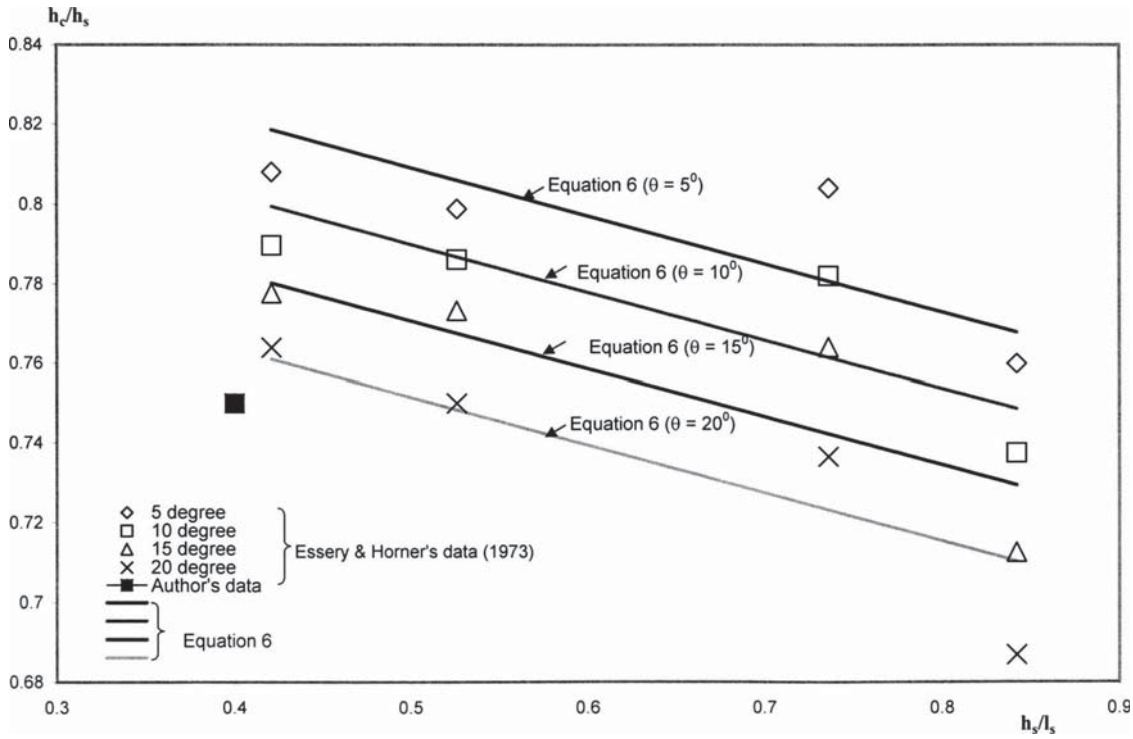

Fig. 2. Effect of inclination of steps on onset of skimming flow

tics of flow over such spillways. Degoutte et al. (1992) carried out model study of gabion-stepped spillways, and found that h_c/h_s at the onset of skimming flow is less than that in the case of an impervious stepped spillway. Chanson (1996) developed an equation for predicting the onset of skimming flow over a stepped spillway, but found that in case of impervious steps, the values of h_c/h_s at the onset of skimming flow obtained by equation and experimental data agree well, whereas a large difference was noted for gabion-stepped spillways. The discussers plotted the values of h_c/h_s at the onset of skimming flow for gabion stepped spillway using experimental data available in the literature as shown in Fig. 1, for comparison with those of stepped spillway. Chinnarasri (2008) suggested the following equation for occurrence of skimming flow on gabion-stepped weir

$$h_c/h_s \geqslant 0.61(h_s/l_s)^{-0.26} \tag{5}$$

which agrees better with the data (Fig. 1).

Hence, the discussers request the authors to comment on comparison of flow characteristics between a stepped-block spillway and stepped spillway with reference to the above points.

The steps provided in the stepped-block spillway are not horizontal but are inclined to the horizontal. The discussers studied the effect of inclination of steps on the onset of skimming flow (Tatewar et al. 1999) and proposed the following equation

$$h_c/h_s = -0.00384\theta - 0.1205(h_s/l_s) + 0.8885 \tag{6}$$

with coefficient of determination $R^2=0.966$, and θ is the angle of inclination of steps with horizontal in degrees.

The steps of a stepped-block spillway resemble the inclined steps of stepped spillway. In the authors' study, the inclination of steps with horizontal is 10°62′. The effect of inclination of steps on the onset of skimming flow is shown in Fig. 2.

From Fig. 2 of the original paper, the authors confirmed that only the two low discharges of the authors' study correspond to transition flow, with all other discharges corresponding to skimming flow. If the comparison is made with curve (1) of Chanson (1994) and curve (2) of Boes and Hager (2003b), only one point corresponds to transition flow. Hence, the discussers are of the opinion that it is difficult to classify the type of flow with reference to a particular equation as shown in Fig. 2 of the original paper.

Acknowledgments

The discussers acknowledge the financial support from the All India Council of Technical Education, New Delhi, India for the construction of stepped-block spillway model for this study (File No. 8023/RID/NPROJ/RPS-6/2004-05).

References

Andre, S. (2004). "High velocity aerated flow on stepped chutes with micro-roughness elements." Ph.D. thesis, EPFL, Lausanne, Switzerland.

Chanson, H. (1996). "Prediction of the transition nappe/skimming flow on a stepped channel." *J. Hydraul. Res.*, 34(3), 421–429.

Chinnarasri, C., Donjadee, S., and Israngkura, U. (2008). "Hydraulic characteristics of gabion-stepped weirs." *J. Hydraul. Eng.*, 134(8), 1147–1153.

Degoutte, G., Peyras, L., and Royet, P. (1992). "Discussion of 'Skimming flows in stepped spillways'." *J. Hydraul. Eng.*, 118(1), 111–113.

Hewlett, H., Baker, R., May, R. W. P., and Pravdivets, Y. P. (1997). "Design of stepped block spillways." *CIRIA, Special Publication No. 142*, CIRIA, London.

Pinheiro, A., and Relvas, A. (2000). "Non-conventional spillways over earth dams. An economical alternative to the conventional chute spillways." *Dam Eng.*, 10(4), 179–196.

Tatewar, S. P., and Ingle, R. N. (1999). "Nappe flow on inclined stepped

spillways." *Journal of Institution of Engineers (India)*, 79(2), 175–179.

Thakare, S. W., Tatewar, S. P., and Ingle, R. N. (2008). "Stepped-block spillway for earthen dam: A case study." *Journal of Institution of Engineers (India)*, 89(8), 3–5.

Closure to "Inception Point and Air Concentration in Flows on Stepped Chutes Lined with Wedge-Shaped Concrete Blocks" by António T. Relvas and Antonio N. Pinheiro

August 2008, Vol. 134, No. 8, pp. 1042–1051.
DOI: 10.1061/(ASCE)0733-9429(2008)134:8(1042)

António T. Relvas, Ph.D.[1]; and António N. Pinheiro[2]

[1]Civil Engineering, Instituto Superior Técnico, Technical University of Lisbon. Rua Eutiquiano Barreto, 77, Apt 402, Manaíra—João Pessoa, CEP 58038-310, Brazil; and, ENGECONSULT, Consultores Técnicos Ltda, Rua Xavier Marques, 94, Aflitos, Recife, CEP 52050-230, Brazil. E-mail: ajtrelvas@gmail.com

[2]Assoc. Prof., Dept. of Civil Engineering, Instituto Superior Técnico, Technical University of Lisbon. IST, SHRHA, Av. Rovisco Pais, 1049-001 Lisboa, Portugal. E-mail: apinheiro@civil.ist.utl.pt

The writers appreciate the comments of the discussers and congratulate them for the work they carried forth on this interesting subject. The related case study of the Chandrabhaga River Project in Maharashtra State of India confirms the cost benefits of the stepped chutes lined with wedge-shaped concrete blocks.

It is worth mentioning that the Barriga dam (rockfill dam), with a stepped chute lined with wedge-shaped concrete blocks for a considerable maximum unit discharge of 7.3 m^2/s, was constructed in Spain (Couto et al. 2007). The Barriga dam stepped chute with wedge-shaped concrete blocks was selected due to cost advantages after a comparative study with a conventional spillway channel in dam abutments as well as in other nonconventional spillways (RCC, rip-rap, and reinforced grass).

As mentioned by the discussers, the writers compared the characteristics of flow (onset of flow regimes, location of inception point and air concentration) on the stepped chutes with concrete blocks with those of the impervious horizontal stepped spillways typical in roller compacted concrete dams (more common in the literature), but also with other studies of stepped chutes lined with wedge-shaped concrete blocks (Frizell et al. 1991; Baker 1994; Gaston 1995). As shown in Fig. 1 of this closure, the water infiltration through the joints and holes of the blocks is much less than the discharge (less than 0.25% for the higher discharges, which represents the skimming flow regimes of more interest for stepped chutes prototypes). This is due to the recirculation of flow from the drainage layer below the blocks to the surface of the blocks, through the blocks holes as represented in Fig. 1. The writers considered therefore that flows in stepped chutes lined with concrete blocks are much more similar to those over impervious steps, and quite different from gabion-stepped spillways, where both step surfaces are pervious and where much higher surface roughness occurs.

Concerning the influence of the step inclination, the discussers present Fig. 2 where they include data from Essery and Horner (1978), where the step inclination θ was considered upward and not downward, as in the writers' work, where the blocks are laid with descending upper faces. In this situation, it does not seem correct to represent the descending angle of the steps' upper surface (10.6°) and compare these results with Essery and Horner (1978) results. For ascending steps, it is expected that h_c/h_s corresponding to the onset of skimming flow decreases with θ for the same ratio h_s/l_s, as it can be observed in Fig. 2.

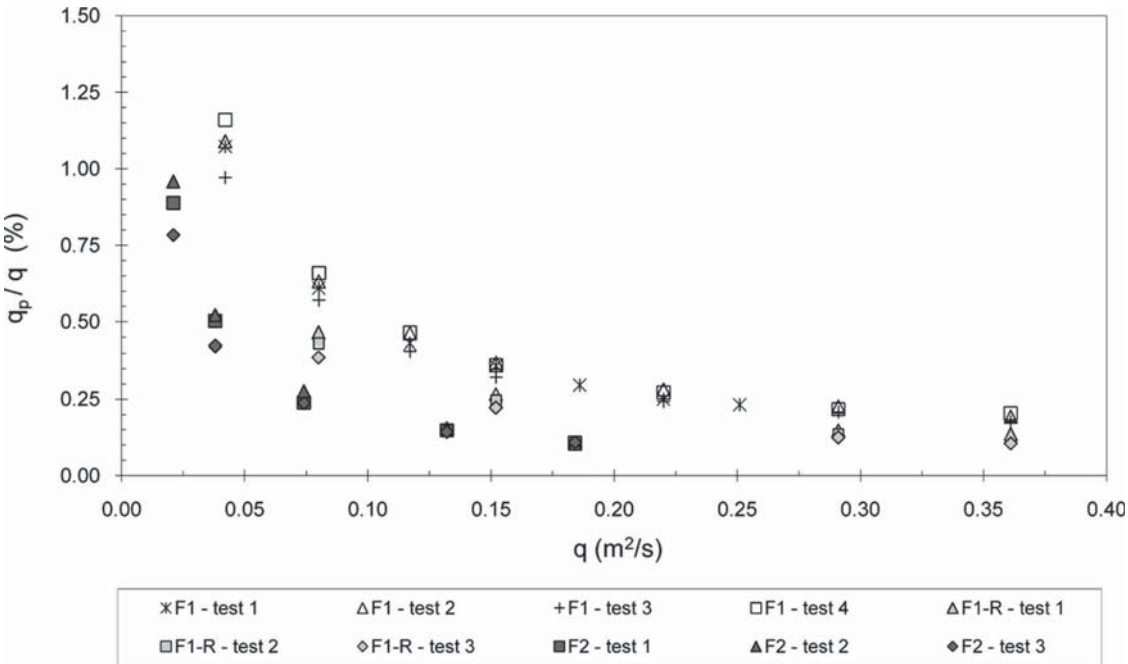

Fig. 1. Variation of unit drainage flow measured at the end of drainage layer, q_p, with flume unit water discharge, q (at flumes F1, F2, and F1-R)

As mentioned in the paper, the writers concluded that the descending angle of the steps' upper surface (10.6°) causes a smoother deflection of the internal jet and less disturbance of the flow. Thus, for equal discharges, compared to chutes with horizontal steps, the onset of skimming flow is expected to occur farther downstream.

The writers agree with the discussers that it is difficult to classify the type of flow with reference to a particular equation as shown in Fig. 2 of the paper. However, it should be noted that the flow observation, as illustrated in Fig. 3 of the paper, confirmed the transition flow pattern for the two lower discharges.

References

Couto, L. T., Magalhães, A. P., Toledo, M. A., and Moya, R. M. (2007). "A new solution for a concrete spillway over a rockfill dam. Hydraulic model study of Barriga in Spain." *Proc., 5th International Conference on Dam Engineering*.

Essery, I. T. S., and Horner, M. W. (1978). "The hydraulic design of stepped spillways." *CIRIA Report, 33*, 2nd Ed., London.